

IMAGE DERAINING VIA SELF-SUPERVISED REINFORCEMENT LEARNING

He-Hao Liao¹, Yan-Tsung Peng¹, Wen-Tao Chu², Ping-Chun Hsieh², and Chung-Chi Tsai³

¹ Dept. of Computer Science, National Chengchi University, Taiwan,

² Dept. of Computer Science, National Yang Ming Chiao Tung University, Taiwan,

³ Qualcomm Technologies, USA

ABSTRACT

The quality of images captured outdoors is often affected by the weather. One factor that interferes with sight is rain, which can obstruct the view of observers and computer vision applications that rely on those images. The work aims to recover rain images by removing rain streaks via Self-supervised Reinforcement Learning (RL) for image deraining (SRL-Derain). We locate rain streak pixels from the input rain image via dictionary learning and use pixel-wise RL agents to take multiple inpainting actions to remove rain progressively. To our knowledge, this work is the first attempt where self-supervised RL is applied to image deraining. Experimental results on several benchmark image-deraining datasets show that the proposed SRL-Derain performs favorably against state-of-the-art few-shot and self-supervised deraining and denoising methods.

Index Terms— Image deraining, self-supervised reinforcement Learning

1. INTRODUCTION

Photos captured outside by personal cameras, dash-cams, surveillance cameras, and other devices can potentially capture scenes of rain, which may obscure the visibility of the images. This can decrease the effectiveness of subsequent computer vision applications, such as object detection and recognition. Therefore, it is essential to have a good method to remove rain from these images so that they can be used effectively.

Image deraining has been much researched. For example, traditional statistical methods separate rain streaks from an image of rain and obtain a clean background [1, 2, 3]. Li *et al.* [1] utilized a priori information to extract rain-related characteristics and applied a Gaussian mixture model to distinguish between background and rain layers. Kang *et al.* [2] applied the dictionary learning, k-means clustering, and sparse coding to separate the non-rain and rain components. Wang *et al.* [3] used dictionary learning to separate rain or snow from the input image. However, these methods rely solely on statistical image priors to restore rain images without much guidance, often resulting in unsatisfying deraining results.

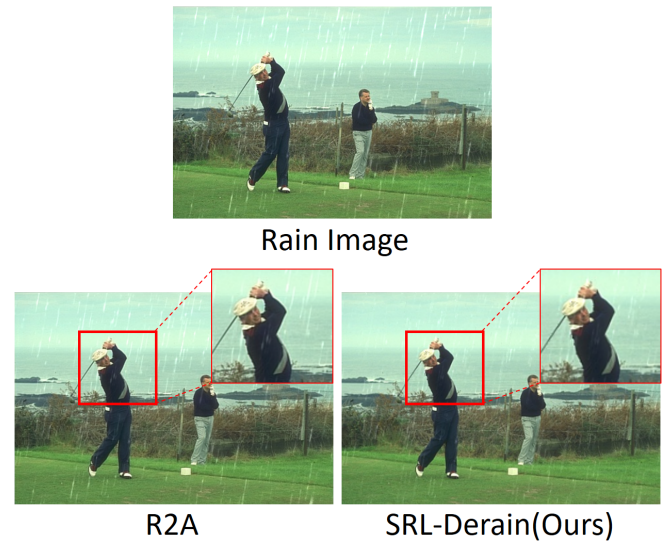


Fig. 1. A comparison of deraining results between R2A [5], a self-supervised learning method, and SRL-Derain, the proposed self-supervised reinforcement-learning method.

Low-level vision tasks have witnessed considerable progress thanks to deep-learning-based methods. In deraining, supervised approaches, leveraging a large amount of rain and rain-free paired training data, allow models to learn rain streaks across various scenes to remove them from rain images. However, collecting paired real-world rain and rain-free images is challenging. As a result, most current methods are trained on synthetic datasets. The domain gap between training and testing sets often leads to suboptimal performance on unseen data or real-world rain images. Wei *et al.* [4] used unpaired images and a generative adversarial network (GAN) with unsupervised learning, but GAN-based models may introduce unexpected artifacts in the results.

The self-supervised deraining task has gained attention recently [5]. However, only a few self-supervised methods have been developed specifically for deraining. Peng *et al.* [5] introduced a self-supervised deraining framework, Rain2Avoid (R2A). They proposed a locally dominant gradient prior (LDGP) to find rain pixels and avoided them upon training with the input rain image. However, its deraining performance is limited by its restoration ability from convo-

lutional neural networks. This paper introduces SRL-Derain, a self-supervised RL approach for image deraining. We adopt dictionary learning as in [2] to locate rain streak pixels and pixel-wise RL agents [6] to take multiple inpainting actions to remove rain streaks from the input image gradually. The reward is calculated based on the pseudo-derained reference [5] and BRISQUE [7] score, a no-reference image quality metric that can be used to evaluate derained results. Figure 1 compares the deraining results of R2A [5] and SRL-Derain. Our self-supervised reinforcement-learning approach removes rain streaks better.

The contributions of this paper are threefold.

- To our best knowledge, this is the first attempt at self-supervised reinforcement learning applied to image deraining.
- We use pseudo-deraining references and a no-reference image quality metric as self-supervised rewards to guide our proposed RL scheme training.
- The experimental results show that the proposed SRL-Derain outperforms state-of-the-art few-shot and self-supervised methods for deraining and denoising.

2. RELATED WORK

2.1. Self-supervised Image Restoration

Although few self-supervised methods have been proposed for image deraining, self-supervised denoising has been well-studied [8, 9, 10]. Ulyanov *et al.* found that the model tended to learn non-noise features more easily during training and proposed the Deep Image Prior (DIP) [8], in which random noise is fed into the neural network supervised with the noisy input image to obtain a denoised image. However, rain features differ from noise, making applying this approach to rain images impractical. N2V [9] and N2S [10] assume that noise in a noisy image is zero-mean and the noise between different pixels is independent. Based on the two assumptions, the network learns the denoised image with averaged noise pixels. Yet, these two assumptions do not apply to rain images and thus cannot effectively remove rain streaks. Peng *et al.* [5] introduced a self-supervised deraining scheme. They predicted the location of rain streaks based on the Locally Dominant Gradient Prior (LDGP) and generated pseudo-derained references for deraining. However, the self-supervised learning scheme using a pure convolutional neural network to learn from imperfect reference images has limitations in restoring derained images. We discovered that RL equipped with a set of conventional filtering tools is a superior method in the Self-Supervised Learning (SSL) regime for image restoration, where only limited information can be provided from a single image.

2.2. Reinforcement-Learning-Based Image Restoration

After the success of Deep Q Learning in RL, it has been broadly applied to tasks such as video game playing, robotics, and autonomous driving. Recently, researchers have further applied RL to solve computer vision tasks. Yu *et al.* [11] addressed three types of image degradation: Gaussian blur, Gaussian noise, and JPEG compression. Park *et al.* [12] uses DQN to train a color enhancement network, which retouches the input image by manipulating the contrast, brightness, or color saturation iteratively. Additionally, Ryosuke *et al.* [6] proposed a multi-agent image restoration framework to solve image denoising, image inpainting, and local color enhancement tasks.

Motivated by the success of SSL, various attempts have augmented RL methods with self-supervision. One major approach is to construct auxiliary tasks based on self-supervised prediction, which typically involves the prediction of forward transition dynamics or inverse dynamics, and use the prediction loss as an additional reward signal for improving the sample efficiency of RL [13]. Another category leverages self-supervised learning to learn informative representations and thereby facilitate the downstream RL, especially for control problems with image-based observations. The principle behind this approach lies in the widely observed empirical evidence that RL from physical state features enjoys better sample efficiency than RL from raw images. For example, [14] proposes CURL, which leverages contrastive learning to extract physical features from raw pixels through joint optimization of the self-supervised and RL losses. This joint optimization framework has also been instantiated through either reconstruction or self-prediction [15]. In addition to joint optimization, self-supervised pre-training has also shown good promise in boosting the data efficiency of downstream RL [16]. Despite the above progress on SSL-augmented RL, one rather underexplored research question is how RL could benefit self-supervised vision tasks.

3. METHODOLOGY

This section details the proposed SRL-Derain. We will start by explaining how we extract rain streaks from the input image and generate pseudo-derained references. After that, we will introduce the multi-agent RL model, which is trained using pseudo-derained references and a no-reference image quality metric. Figure 2 depicts the overall flowchart of the proposed SRL-Derain.

3.1. Generation of the Rain Mask and Pseudo-derained References

Rain Mask Generation. There are several methods [17, 5] to separate rain streaks from rain images. Jiang *et al.* [17] calculated the discriminatively intrinsic prior using the unidirectional total variation of the rain direction, determined based

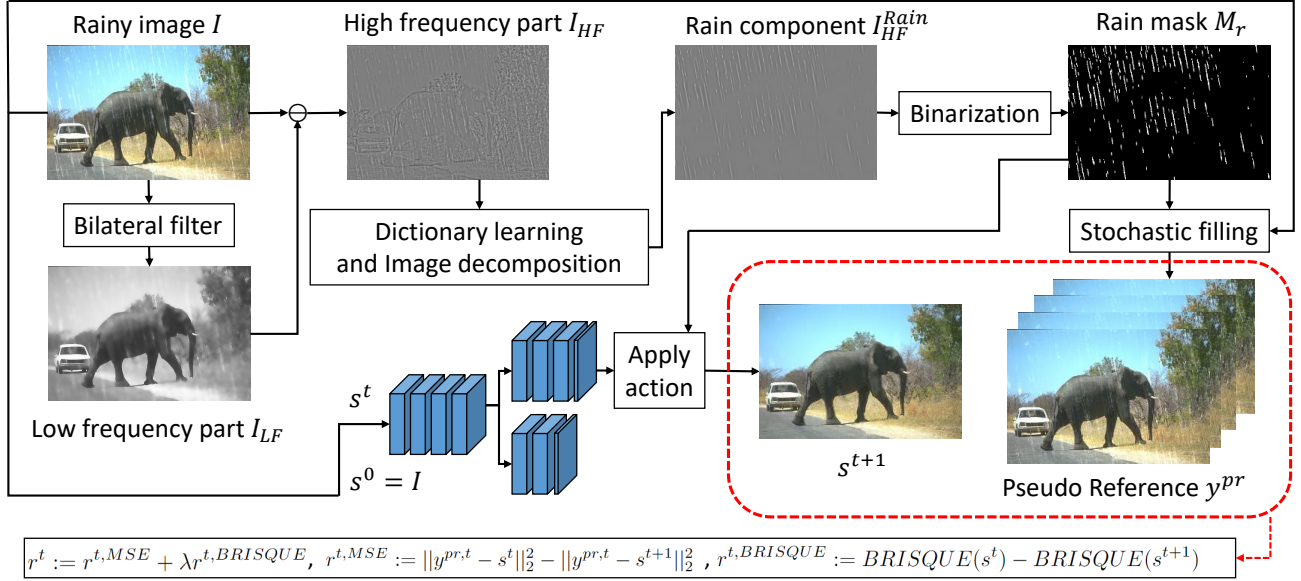


Fig. 2. The flowchart of the proposed self-supervised RL-based deraining scheme. To locate rain pixels and generate the rain mask, we utilize bilateral filtering to extract the high-frequency part I_{HF} from the input rain image and decompose the rain components via dictionary learning [2]. The RL model progressively fills the rain pixels in the rain image based on the rain mask. Note that $r^t \in R^{H \times W}$ is the total reward map for the state s^t at the time step t .

on the differences between consecutive video frames. However, it is not suitable for single-image deraining. Peng *et al.* [5] proposed Locally Dominant Gradient Prior (LDGP), calculating the Histogram of Oriented Gradients (HoGs) for each local region of a rain image and performing a majority vote to determine the rain-streak angle. After that, they extracted the rain streaks based on the angle using image morphological operations. However, it can only find the rain streaks at one angle. By contrast, we adopt dictionary learning as in [2] to locate rain pixels, which we call Rain Dictionary Prior (RDP). First, using a bilateral filter, we decompose the rain image into low- and high-frequency parts I_{LF} and I_{HF} . Next, we construct a dictionary $D \in R^{n \times m}$ for I_{HF} using online dictionary learning [18] as:

$$\operatorname{argmin}_{D, \theta_d^i} \frac{1}{N_p} \sum_{i=1}^{N_p} \left(\frac{1}{2} \|y_{HF}^i - D\theta_d^i\|_2^2 + \lambda_d \|\theta_d^i\|_1 \right), \quad (1)$$

where $y_{HF}^i \in R^n$ is $p \times p$ overlapped patches centered at each pixel obtained from I_{HF} and vectorized with size $n = p^2$, N_p is the number of total patches extracted, θ_d^i is the sparse coefficients for the dictionary D to construct y_{HF}^i , and m is the number of atoms in the dictionary. Next, to extract rain-related atoms from the dictionary, each y_{HF}^i is described by the HOG descriptor and classified into two clusters by the K-means algorithm. The cluster with the lower variance represents the rain-related atoms since rain streaks are geometrically simple, as suggested in [2]. Then, we utilize the rain-related atoms in the dictionary to reconstruct the rain compo-

nent I_{HF}^{Rain} , followed by binarization to obtain the rain mask M_r as the RDP.

Pseudo-derained Reference Generation. To train our multi-agent RL model in a self-supervised manner, we use the rain mask generated by R2A [5] to create pseudo-derained references. We then identify rain pixels from the rain mask and replace them with non-rain pixels around them in a stochastic manner. This means that for each rain pixel indicated by the computed RDP, a non-rain pixel in its neighborhood is randomly selected to generate a pseudo-derained reference y^{pr} for the RL's reward function later.

3.2. RL-based Self-supervised Deraining Scheme

We propose to cast image deraining as an RL problem with self-supervised rewards. Specifically: (i) Regarding the RL formulation, we adopt the pixel-wise control as in pixelRL [6], an RL-based image enhancement framework with one agent for each pixel based on the Asynchronous Advantage Actor-Critic (A3C) algorithm, to remove rain streaks from the input rain image, where the rain pixels are progressively restored with a clean background. Let s_i^t , a_i^t , and r_i^t denote the image state, the action, and the self-supervised reward of the i -th pixel at each step t of the RL-based deraining episode, respectively. Let $\gamma \in [0, 1)$ be the discount factor. Built on the A3C method, SRL-Derain consists of a policy network $\pi_i(\cdot|s; \theta_p)$ and a value network $V(\cdot|s; \theta_v)$, which are parameterized by θ_p and θ_v , respec-

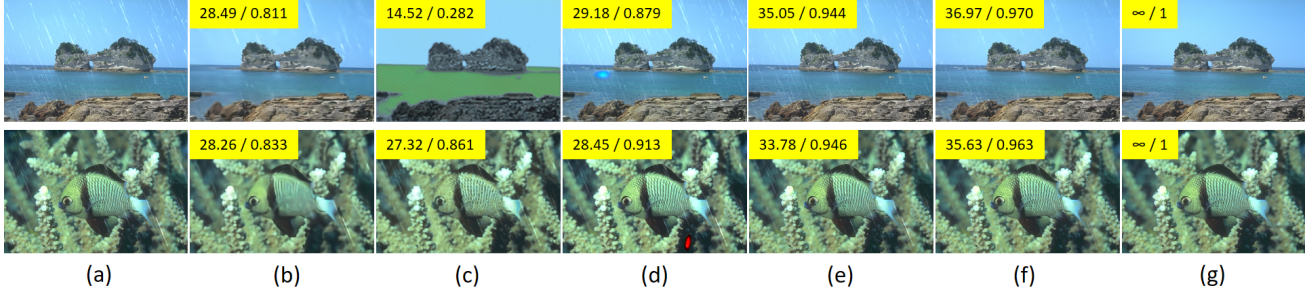


Fig. 3. Qualitative comparisons on Rain100L with PSNR/SSIM values shown on the results. (a) Input images, and the derained results obtained using (b) DIP [8], (c) N2S [10], (d) N2V [9], (e) R2A [5], and (f) Ours. (g) GT images.

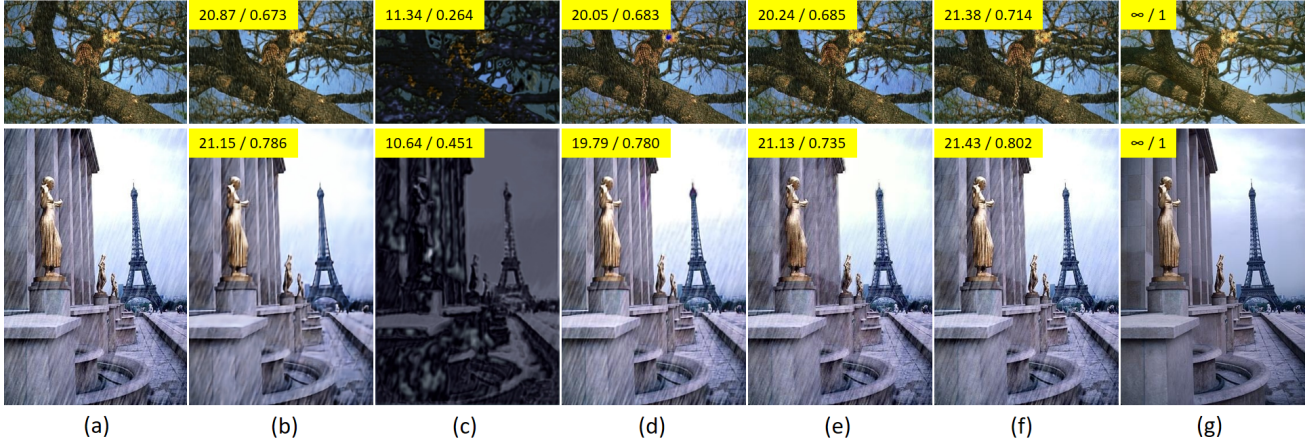


Fig. 4. Qualitative comparisons on Rain800 with PSNR/SSIM values shown on the results. (a) Input images, and the derained results obtained using (b) DIP [8], (c) N2S [10], (d) N2V [9], (e) R2A [5], and (f) Ours. (g) GT images.

tively. Let $\pi_i(\cdot|s; \theta_p)$ denote the action distribution of the i -th pixel at state s under the policy parameter θ_p . The policy and value networks are iteratively updated by taking gradient steps of the corresponding loss functions defined as follows. In each iteration, we collect the trajectory of each pixel $\{s_i^1, a_i^1, r_i^1, \dots, s_i^T, a_i^T, r_i^T\}$ and compute the value loss and the policy loss as

$$L_v(\theta_v) := \sum_{t=1}^T \frac{1}{N} \sum_{i=1}^N (R_i^t - V(s_i^t; \theta_v))^2, \quad (2)$$

$$L_p(\theta_p) := - \sum_{t=1}^T \sum_{i=1}^N \log \pi(a_i^t | s_i^t; \theta_p) A(a_i^t, s_i^t), \quad (3)$$

where R_i^t and $A(a_i^t, s_i^t)$ denotes the n -step return and the n -step return with baseline defined as

$$R_i^t := r_i^t + \gamma r_i^{t+1} + \gamma^2 r_i^{t+2} + \dots + \gamma^n V(s_i^{t+n}; \theta_v), \quad (4)$$

$$A(a_i^t, s_i^t) := R_i^t - V(s_i^t; \theta_v). \quad (5)$$

Following [6], we can simultaneously train multiple pixel-wise agents using convolution neural networks.

To guide the training of the RL model, the proposed self-supervised rewards include a conventional mean-square-error-based difference between the state of the i -th agent (the

i -th pixel in the intermediate derained image) and the corresponding pixel in the pseudo-derained reference $y_i^{pr,t}$ at the time step t , denoted as $r_i^{t,MSE}$ and the proposed no-reference quality metric reward, $r_i^{t,BRISQUE}$, described as follows:

$$r_i^{t,MSE} := \|y_i^{pr,t} - s_i^t\|_2^2 - \|y_i^{pr,t} - s_i^{t+1}\|_2^2; \quad (6)$$

$$r_i^{t,BRISQUE} := BRISQUE(s^t) - BRISQUE(s^{t+1}); \quad (7)$$

$$r_i^t := r_i^{t,MSE} + \lambda r_i^{t,BRISQUE}, \quad (8)$$

where $BRISQUE(s^t)$ returns the BRISQUE score of s^t and λ is a hyperparameter that balances between the two rewards. Since producing the pseudo-derained reference $y^{pr,t}$ is a stochastic process, the reference must be randomly sampled at each time step.

4. EXPERIMENTS

Datasets: To evaluate the deraining performance, we use four public deraining benchmark datasets, consisting of Rain100L [19], Rain800 [20], and DDN-SIRR [21]. Rain100L and Rain800 are synthetic datasets, and DDN-SIRR [21] contains 14,000 synthetic images and 147 real-world rain images. Here, we use the Rain100L test set, Rain800 test set, and all real-world DDN-SIRR images (dubbed with

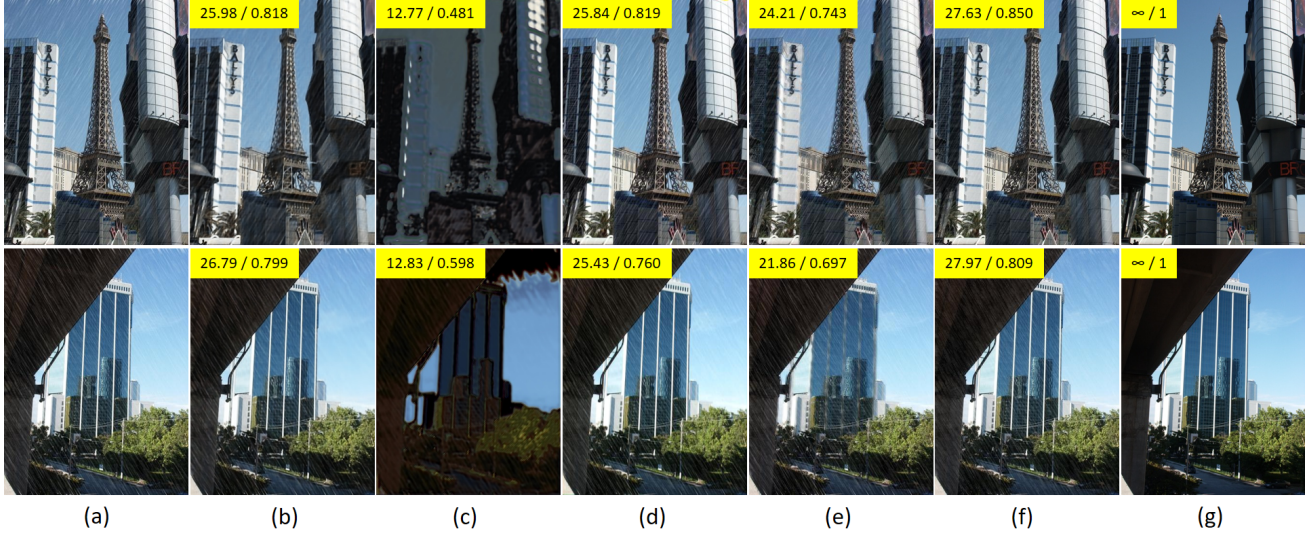


Fig. 5. Qualitative comparisons on DDN-SIRR_syn with PSNR/SSIM values shown on the results. (a) Input images, and the derained results obtained using (b) DIP [8], (c) N2S [10], (d) N2V [9], (e) R2A [5], and (f) Ours. (g) GT images.

Table 1. The inpainting action set for SRL-Derain as used in [6]

Index	Action	Filter Size	Parameter
1	box filter	5×5	-
2	bilateral filter	5×5	$\sigma_c = 1.0, \sigma_s = 5$
3	bilateral filter	5×5	$\sigma_c = 0.1, \sigma_s = 5$
4	median filter	5×5	-
5	gaussian filter	5×5	$\sigma = 1.5$
6	gaussian filter	5×5	$\sigma = 0.5$
7	pixel value += 1	-	-
8	pixel value -= 1	-	-
9	do nothing	-	-

DDN-SIRR_real) and 400 images randomly sampled from the synthetic DDN-SIRR set (dubbed with DDN-SIRR_syn) as practiced in [22].

Implementation Details. We train the RL agents using the Adam optimizer for 100 episodes with the initial learning rate starting from 1×10^{-3} and multiplied by $(1 - \frac{episode}{max_episode})^{0.9}$ at each episode, where $max_episode$ is set to 150. The length of each episode t_{max} is set to 15. The action set is listed in Table 1. The λ in Eq. 8 is set to 0.025 empirically. The model is implemented in Python with Chainer and trained on a computer equipped with an Intel Xeon Silver 4210 CPU and a single ASUS TURBO RTX 3090 GPU with 24G memory.

Image Quality Metrics and Compared Methods. For synthetic data with the Ground Truth (GT), we evaluate the performance with PSNR and SSIM. On the other hand, we use no-reference image quality metrics, the Blind/Referenceless Image Spatial Quality Evaluator (BRISQUE) [7], for real-world rain images without their GT. BRISQUE is a score calculated based on the extracted Natural Scene Statistics. A larger value for PSNR or SSIM means better performance, while a smaller value for BRISQUE indicates better quality. We compare our SRL-Derain with state-of-the-art deraining

Table 2. Evaluation results on Rain800, DDN-SIRR_syn and DDN-SIRR_real. The best scores are in bold, and the second best is underlined.

Method	Rain800		DDN-SIRR_syn		DDN-SIRR_real
	PSNR \uparrow	SSIM \uparrow	PSNR \uparrow	SSIM \uparrow	BRISQUE \downarrow
Kang’s [2]	21.20	0.730	22.65	0.712	122.063
David’s [23]	18.95	0.663	19.18	0.681	38.581
DIP [8]	22.24	0.684	23.49	0.725	60.540
N2S [10]	19.11	0.506	19.06	0.496	89.041
N2V [9]	21.75	0.659	22.81	0.712	39.702
R2A [5]	<u>22.76</u>	0.732	<u>24.61</u>	<u>0.784</u>	30.141
SRL-Derain (Ours)	23.13	0.723	24.91	0.789	29.308

and denoising approaches, including a dictionary-learning-based deraining method (Kang’s [2]), a prior-based conventional deraining method (David’s [23]), a semi-supervised deraining method (Wei’s [21]), a few-shot self-supervised deraining method (FLUID [22]), three self-supervised denoising methods (DIP [8], N2V [9], and N2S [10]), and self-supervised deraining method (R2A [5]).

Quantitative Analysis. We compare with existing methods [2, 23, 8, 10, 9, 5], on the Rain800, DDN-SIRR_syn, and DDN-SIRR_real datasets, as presented in Table 2. Our method performs favorably against the compared methods on these datasets. Additionally, we compare our approach with [2, 23, 8, 10, 9, 5], the semi-supervised deraining method Wei’s [21], and the few-shot self-supervised deraining method FLUID [22] with 1-shot, 3-shot, and 5-shot settings on Rain100L. Table 3 shows our SRL-Derain achieves the best results, even better than FLUID [22] with 3-shot or 5-shot settings (3 or 5 more training images used).

Qualitative Analysis. We also compare the derained results of our method with those using the compared self-supervised denoising methods [8, 10, 9] and self-supervised deraining approach [5]. Figure 3 shows some examples of deraining results on the Rain100L testing set, where DIP [8] seems

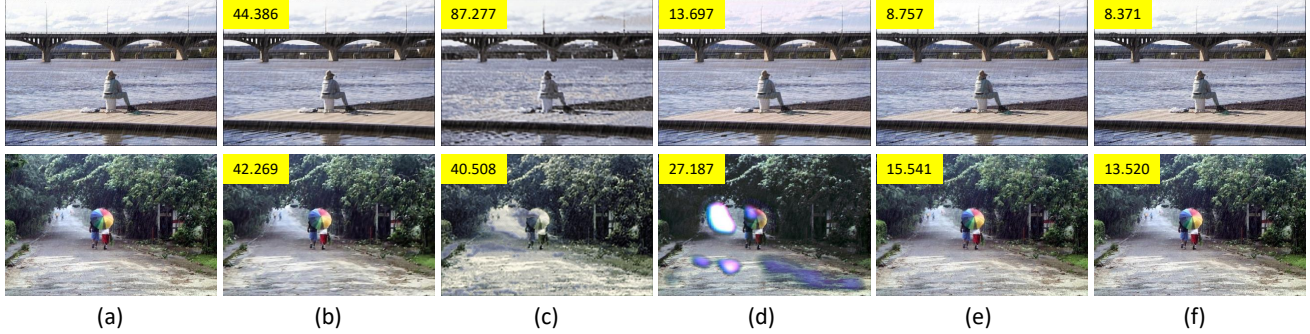


Fig. 6. Qualitative comparisons on DDN-SIRR_real with BRISQUE values shown on the results. (a) Input images, and the derained results obtained using (b) DIP [8], (c) N2S [10], (d) N2V [9], (e) R2A [5], and (f) Ours.

Table 3. Evaluation results on Rain100L. Note that the results of Wei’s [21] and FLUID (1-, 3-, and 5-shot) are directly excerpted from [22].

Rain100L	Kang’s	David’s	DIP	N2S	N2V	Wei’s	FLUID (1)	FLUID (3)	FLUID (5)	R2A	SRL-Derain (Ours)
PSNR \uparrow	24.46	19.94	24.98	20.20	21.74	23.77	23.87	25.54	26.87	<u>29.17</u>	29.86
SSIM \uparrow	0.713	0.744	0.704	0.498	0.648	0.775	0.772	0.826	0.862	<u>0.887</u>	0.906

only to blur the images. N2S [10] removes most rain streaks but causes color distortions. N2V [9] removes partial rain but introduces color artifacts. R2A [5] also removes most rain, whereas the proposed SRL-Derain works the best. Figure 4 and Figure 5 demonstrate two derained results on the Rain800 testing set and the DDN-SIRR_syn testing set. As can be seen, we have similar observations to those for Figure 3, where SRL-Derain also performs favorably. The PSNR and SSIM values shown in the results can also validate these visualizations. Figure 6 shows the results on the DDN-SIRR_real dataset, where the abovementioned observations for the synthetic rain images can also apply. We can find that R2A and the proposed SRL-Derain work comparably, both of which restore the rain images nicely.

Ablation Study and Analysis. In this section, we conduct an ablation study on two designs we adopt to verify their effectiveness. First, to be fair in comparison with self-supervised denoising methods, which do not have a priori knowledge about rain like R2A [5] (w/ LDGP) and our SRL-Derain (w/ RDP), we provide those methods with the Ground Truth (GT) rain mask for them to not denoise non-rain pixels, which may cause unwanted blur. Note that the study uses the Rain100L training set since it has the GT rain masks. Table 4 shows the self-supervised denoising methods (N2V and DIP) using the GT rain mask to avoid smoothing non-rain pixels perform better than without the mask. R2A with the GT mask also works better than its original LDGP. As also can be seen, our SRL-Derain using LDGP achieves higher PSNR/SSIM values than R2A, showing our proposed self-supervised RL scheme outperforms the SSL deraining method. SRL-Derain using the GT mask works better than the other methods with the setting. In addition, Table 5 verifies the effectiveness of adding the no-reference quality metric, BRISQUE, to the reward function on the Rain100L testing set, where SRL-Derain using BRISQUE as a reward can indeed improve the BRISQUE score. At last,

Table 4. Ablation on effects of the rain mask provided for self-supervised methods.

Rain100L_train		
Rain Mask	PSNR \uparrow	SSIM \uparrow
N2V [9]	22.74	0.654
N2V w/ GT Mask	25.99	0.822
DIP [8]	24.79	0.709
DIP w/ GT Mask	27.76	0.781
R2A w/ LDGP [5]	28.79	0.895
R2A w/ GT Mask	<u>31.08</u>	<u>0.927</u>
SRL-Derain w/ LDGP	29.09	0.895
SRL-Derain w/ RDP	29.82	0.906
SRL-Derain w/ GT Mask	32.50	0.929

we can train SRL-Derain on multiple images in an SSL manner. In our experiment, SRL-Derain can achieve 29.93dB in PSNR, higher than R2A [5] by 0.88dB, and our average inference time for running 15 steps is 1.05 seconds.

5. CONCLUSIONS

This paper presents SRL-Derain, a self-supervised RL scheme for image deraining. By incorporating pseudo-derained references and a no-reference image quality metric as self-supervised rewards, we can successfully train an RL model to progressively derain the input rain image. The experimental results indicated that the proposed method performed favorably against the SOTA few-shot deraining and self-supervised denoising and deraining methods. We hope this work can inspire future research on using self-supervised RL for low-level vision tasks.

Table 5. Ablation on the BRISQUE reward in the proposed SRL-Derain.

Rain100L_test			
Reward	PSNR \uparrow	SSIM \uparrow	BRISQUE \downarrow
w/o BRISQUE	29.86	0.904	11.891
w/ BRISQUE	29.86	0.906	10.071

6. REFERENCES

- [1] Yu Li, Robby T Tan, Xiaojie Guo, Jiangbo Lu, and Michael S Brown, "Rain streak removal using layer priors," in *Proc. Conf. Computer Vision and Pattern Recognition*, 2016.
- [2] Li-Wei Kang, Chia-Wen Lin, and Yu-Hsiang Fu, "Automatic single-image-based rain streaks removal via image decomposition," *IEEE Trans. on Image Processing*, 2011.
- [3] Yinglong Wang, Shuaicheng Liu, Chen Chen, and Bing Zeng, "A hierarchical approach for rain or snow removing in a single color image," *IEEE Trans. on Image Processing*, 2017.
- [4] Yanyan Wei, Zhao Zhang, Yang Wang, Mingliang Xu, Yi Yang, Shuicheng Yan, and Meng Wang, "Deraincyclegan: Rain attentive cyclegan for single image deraining and rainmaking," *IEEE Trans. on Image Processing*, 2021.
- [5] Yan-Tsung Peng and Wei-Hua Li, "Rain2avoid: Self-supervised single image deraining," in *Proc. Int'l Conf. Acoustics, Speech, and Signal Processing*, 2023.
- [6] Ryosuke Furuta, Naoto Inoue, and Toshihiko Yamasaki, "Fully convolutional network with multi-step reinforcement learning for image processing," in *Proc. Nat'l Conf. Artificial Intelligence*, 2019.
- [7] Anish Mittal, Anush Krishna Moorthy, and Alan Conrad Bovik, "No-reference image quality assessment in the spatial domain," *IEEE Trans. on Image Processing*, 2012.
- [8] Dmitry Ulyanov, Andrea Vedaldi, and Victor Lempitsky, "Deep image prior," in *Proc. Conf. Computer Vision and Pattern Recognition*, 2018.
- [9] Alexander Krull, Tim-Oliver Buchholz, and Florian Jug, "Noise2void-learning denoising from single noisy images," in *Proc. Conf. Computer Vision and Pattern Recognition*, 2019.
- [10] Joshua Batson and Loic Royer, "Noise2self: Blind denoising by self-supervision," in *Proc. Int'l Conf. Machine Learning*, 2019.
- [11] Ke Yu, Chao Dong, Liang Lin, and Chen Change Loy, "Crafting a toolchain for image restoration by deep reinforcement learning," in *IEEE Trans. on Pattern Analysis and Machine Intelligence*, 2018.
- [12] Jongchan Park, Joon-Young Lee, Donggeun Yoo, and In So Kweon, "Distort-and-recover: Color enhancement using deep reinforcement learning," in *IEEE Trans. on Pattern Analysis and Machine Intelligence*, 2018.
- [13] Evan Shelhamer, Parsa Mahmoudieh, Max Argus, and Trevor Darrell, "Loss is its own reward: Self-supervision for reinforcement learning," in *International Conference on Learning Representations Workshop*, 2017.
- [14] Michael Laskin, Aravind Srinivas, and Pieter Abbeel, "CURL: Contrastive unsupervised representations for reinforcement learning," in *Proc. Int'l Conf. Machine Learning*, 2020, pp. 5639–5650.
- [15] Max Schwarzer, Ankesh Anand, Rishab Goel, R Devon Hjelm, Aaron Courville, and Philip Bachman, "Data-efficient reinforcement learning with self-predictive representations," in *Proc. Int'l Conf. Learning Representations*, 2021.
- [16] Irina Higgins, Arka Pal, Andrei Rusu, Loic Matthey, Christopher Burgess, Alexander Pritzel, Matthew Botvinick, Charles Blundell, and Alexander Lerchner, "Darla: Improving zero-shot transfer in reinforcement learning," in *Proc. Int'l Conf. Machine Learning*, 2017.
- [17] Tai-Xiang Jiang, Ting-Zhu Huang, Xi-Le Zhao, Liang-Jian Deng, and Yao Wang, "Fastderain: A novel video rain streak removal method using directional gradient priors," *IEEE Trans. on Image Processing*, 2018.
- [18] Julien Mairal, Francis Bach, Jean Ponce, and Guillermo Sapiro, "Online learning for matrix factorization and sparse coding.," *Journal of Machine Learning Research*, 2010.
- [19] Wenhan Yang, Robby T Tan, Jiashi Feng, Jiaying Liu, Zongming Guo, and Shuicheng Yan, "Deep joint rain detection and removal from a single image," in *Proc. Conf. Computer Vision and Pattern Recognition*, 2017.
- [20] He Zhang, Vishwanath Sindagi, and Vishal M Patel, "Image de-raining using a conditional generative adversarial network," *IEEE Trans. on Circuits and Systems for Video Technology*, 2019.
- [21] Wei Wei, Deyu Meng, Qian Zhao, Zongben Xu, and Ying Wu, "Semi-supervised transfer learning for image rain removal," in *Proc. Conf. Computer Vision and Pattern Recognition*, 2019.
- [22] Shyam Nandan Rai, Rohit Saluja, Chetan Arora, Vineeth N Balasubramanian, Anbumani Subramanian, and CV Jawahar, "Fluid: Few-shot self-supervised image deraining," in *Proc. of the IEEE/CVF Winter Conf. on Applications of Computer Vision*, 2022.
- [23] David Eigen, Dilip Krishnan, and Rob Fergus, "Restoring an image taken through a window covered with dirt or rain," in *Proc. Int'l Conf. Computer Vision*, 2013.